

Lawrence Berkeley National Laboratory

Lawrence Berkeley National Laboratory

Title

Ultra-peripheral collisions of relativistic heavy ions

Permalink

<https://escholarship.org/uc/item/81s50015>

Authors

Klein, S.
STAR Collaboration

Publication Date

2001

Ultra-peripheral collisions of relativistic heavy ions

S. Klein for the STAR Collaboration

70-319 LBNL, Berkeley, CA, 94720 USA

Abstract.

We report the first observation of exclusive ρ production in ultra-peripheral collisions at RHIC. The ρ are produced electromagnetically at large impact parameters where no hadronic interactions occur. The produced ρ have a small perpendicular momentum, consistent with production that is coherent on both the photon emitting and scattering nuclei. We observe both exclusive ρ production, and ρ production accompanied by electromagnetic dissociation of both nuclei. We discuss models of vector meson production and the correlation with nuclear breakup. We also observe e^+e^- pair production in these ultra-peripheral collisions.

INTRODUCTION

Vector mesons can be produced by photonuclear interactions in ultra-peripheral heavy ion collisions (UPC). The electromagnetic interactions occur at impact parameters b larger than twice the nuclear radius R_A , where no hadronic interactions can occur[1]. In these UPCs, the electromagnetic field of one nucleus acts as almost-real photon field, following the Weizsäcker-Williams approach. These photons can fluctuate into a quark-antiquark pair, which can scatter elastically from the other nucleus, emerging as a real vector meson. The photons can also fluctuate into virtual $\pi^+\pi^-$ pairs, with one of the pions scattering from the other nucleus and emerging as a real pion pair.

Purely electromagnetic interactions also occur. At energy scales above \hbar/R_A , for most purposes, these may be described as two-photon interactions, although 3 (or more) photon interactions are also possible[2]. These reactions can produce e^+e^- , $\mu^+\mu^-$ and $\tau^+\tau^-$ pairs, scalar or tensor mesons, and meson pairs[3]. Since the photons couple to charge, the production rate is a sensitive test of the internal charge content of mesons, and can be used to rule out glueball candidates.

UPCs occur at moderate impact parameters, $2R_A < b < \gamma \hbar c/M_V$ where M_V is the vector meson mass and γ the (lab frame) Lorentz boost. Because the electromagnetic fields are so strong, additional photonuclear interactions may accompany the vector meson production. In addition to the ρ producing photon, the nuclei may exchange one or more additional photons which may excite the target nuclei into a giant dipole resonance or higher excitation. When the excited nuclei decay, they emit one or more neutrons.

We report the first observation of ρ production in UPCs, both with and without nuclear excitation. We also observe e^+e^- pairs produced in UPCs. These reactions were observed in $Au + Au$ collisions at a center of mass energy $\sqrt{s_{NN}} = 130$ GeV at the Relativistic Heavy Ion Collider (RHIC) by the Solenoidal Tracker at RHIC (STAR) detector. Figure 1 shows a typical event: two charged particles are visible in an otherwise empty detector. The particles are roughly back-to-back, showing that the pair has a small transverse momentum p_T .

RATES

The rates for exclusive ρ production may be calculated using data on $\gamma p \rightarrow \rho p$ collected from HERA and fixed target experiments. The photon flux is given by the Weizsäcker-Williams virtual photon method. The cross section to produce a vector meson V , $\sigma(\gamma A \rightarrow VA)$, is determined by a Glauber calculation using the $\gamma p \rightarrow Vp$ data as input. The calculated $\sigma(\gamma A \rightarrow VA)$ cross sections[4] agree with data from lower energy fixed target experiments. For less-well studied mesons, the measured vector meson rates may be used to determine the meson-nucleon interaction cross

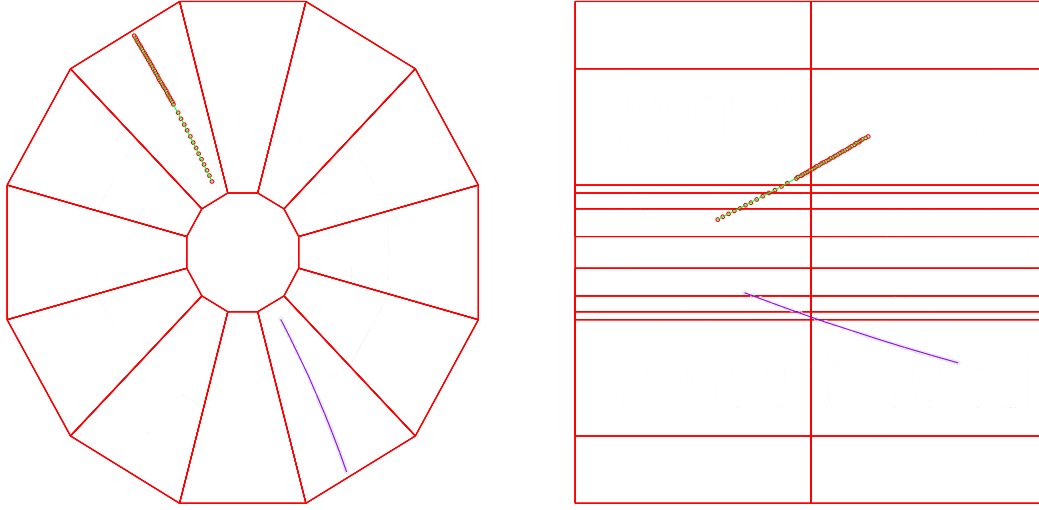


FIGURE 1. End and side views of a typical ρ candidate event in the STAR TPC. The candidate tracks are almost back-to-back radially, but boosted longitudinally.

sections.

The production cross section at a given photon energy k (in the lab frame) maps into the rapidity η of the final state vector meson: $y = 1/2 \ln(2k/M_V)$. A photon with a lab-frame energy $k = M_V/2$ is Lorentz boosted to an energy γM_V in the target frame, so the γp center of mass energies are comparable to those reached at Fermilab fixed-target experiments, somewhat below those reached at HERA.

The total cross section is the integral over k of the photon flux times $\sigma(\gamma A \rightarrow VA)$. For gold collisions at $\sqrt{s_{NN}} = 130$ GeV the ρ production cross section is expected to be about 400 mb, 5% of the total hadronic cross section.

A $\pi\pi$ final state may be produced directly or through the ρ . The amplitudes for ρ production, A , and direct $\pi\pi$ production, B , interfere and[5]

$$\frac{d\sigma}{dM_{\pi\pi}} = \left| \frac{A\sqrt{M_{\pi\pi}M_\rho\Gamma_\rho}}{M_{\pi\pi}^2 - M_\rho^2 + iM_\rho\Gamma_\rho} + B \right|^2 \quad (1)$$

where the ρ width is corrected for the increasing phase space as $m_{\pi\pi}$ increases. The ρ component undergoes a 180° phase shift at M_ρ , so the interference skews the ρ peak shape, enhancing production for $M_{\pi\pi} < M_\rho$ and suppressing the spectrum for $M_{\pi\pi} > M_\rho$.

These UPCs are characterized by final states with small p_T because of the coherent coupling. The meson p_T comes from the photon, $p_T(\gamma) \sim \hbar/b$ and the p_T acquired in the scattering, about \hbar/R , added in quadrature. Vector meson production can occur at either of the nuclei; because the strong force has a short range, the production must be inside or very near the nuclei. Because it is impossible to determine which nucleus was the source, the amplitudes from the two production sites (ions) interfere, reducing the number of ρ with $p_T < \hbar/b$ [6]. Because the short-lived ρ decay before they travel the distance b , the interference is sensitive to the post-decay wave function, and can be used for tests of quantum mechanics.

Electron-positron pairs may be produced in UPCs by purely electromagnetic processes. Although the coupling is large ($Z\alpha \sim 0.6$), in the kinematic range accessible to STAR, higher order effects are likely to be small, and the cross section is calculable based on the collision of two almost-real virtual photons[1].

Photon exchange can also excite one or both nuclei[7]. Collective excitations, such as the Giant Dipole Resonance, are possible, along with higher energy incoherent photonuclear interactions involving hadron production. Calculations indicate that, in mutual Coulomb dissociation, the two excitations are likely to occur independently, via two separate photons. The cross section for mutual coulomb exchange is sizable, around 3.6 barns at $\sqrt{s_{NN}} = 130$ GeV[8]. This process may be used as a luminosity monitor. Mutual excitation also 'tags' events with low impact parameters.

The impact parameter dependence depends only on the photon flux variation. The flux at a given b is given in the Weizsäcker-Williams formalism[9]. Multiple photons from a single nucleus are emitted independently of each other[10]. As long as there is no interference between final states, the individual interactions are independent events,

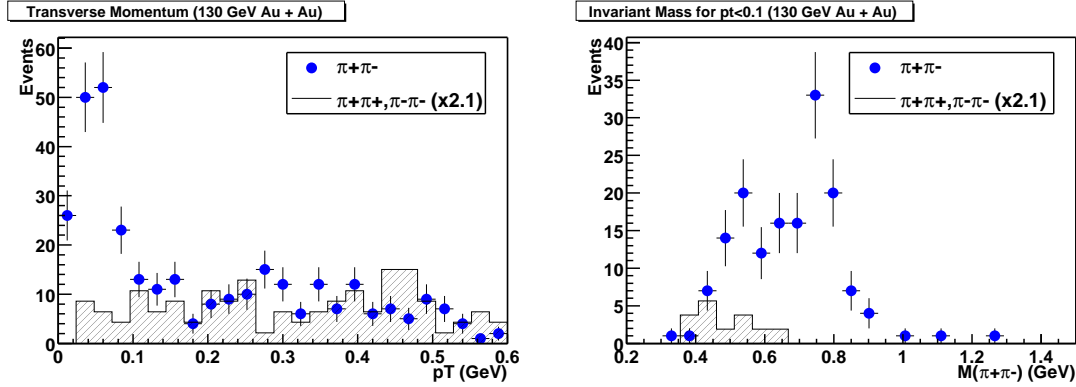


FIGURE 2. (a) The p_T spectrum of topology triggered 2-track events. (b) The $m_{\pi\pi}$ spectrum of 2-track events with $p_T < 100$ MeV/c. The points are oppositely charged pairs, while the histograms are the like-sign background, scaled up by a factor of 2.1.

with the cross section for multiple interactions given by an integration of the joint probabilities over transverse space:

$$\sigma = \int d^2b P_\rho(b) P_{2EXC}(b) [1 - P_{HAD}(b)]. \quad (2)$$

where $P_\rho(b)$ is the probability of ρ production and $P_{2EXC}(b)$ is the probability of mutual nuclear excitation. There are some Feynman diagrams for which factorization doesn't apply. For example, when photon emission excites the emitting nucleus, factorization fails. These processes have been studied for two-photon UPCs, and the non-factorizing amplitudes were found to be small[11]. It seems likely that a similar independence holds for photonuclear interactions.

DATA COLLECTION, TRIGGERING AND ANALYSIS

The STAR detector reconstructs charged particles using a 4.2 meter long time projection chamber (TPC)[12] in a 0.25 T solenoidal magnetic field. The TPC has an inner radius of 50 cm, and an outer radius of 2 m. The charged particle pseudorapidity (η) acceptance depends on the position of the interaction. For the data discussed here, the interactions were radially within a few cm of the center of the TPC, but spread longitudinally (in z), with $\sigma_z = 90$ cm. Tracks originating near $z = 0$ (the center of the TPC) were tracked for $|\eta| < 1.5$. The momentum resolution was about $\Delta p/p = 2\%$. Tracks with $p_T > 100$ MeV/c were reconstructed with good efficiency. Particles were identified by their energy loss (dE/dx) in the TPC. For low-multiplicity final states, the dE/dx resolution was about 8%.

The TPC is surrounded by a cylindrical central trigger barrel (CTB). For tracks originating near $z = 0$, it is sensitive to $|\eta| < 1.0$. This barrel consists of 240 scintillator slats, each covering $\Delta y = 0.5$ by $\Delta\phi = \pi/30$.

Two zero degree calorimeters (ZDCs) at $z = \pm 18.25$ meters from the interaction point detect neutrons from nuclear breakup. These calorimeters have $> 99\%$ acceptance for single neutrons from nuclear breakup[13].

The initial trigger decision uses lookup tables and field programmable gate arrays to initiate TPC readout about 1.5 μ s after the collision. TPC readout took 10 msec, allowing for up to 100 events/sec to be read out (at 100% downtime). A higher level filter uses on-line track reconstruction by a small processor farm [14] to remove unwanted events with vertices outside the beam interaction region.

EXCLUSIVE ρ PRODUCTION

Two separate triggers were used to study ρ production. The first ('topology') trigger selected events with a small number of tracks detected by the CTB. It divided the CTB into 4 azimuthal quadrants, and required a hit in the opposing 'North' and 'South' quadrants. Events with hits in the top or bottom quadrants were vetoed as probable cosmic rays. We took 7 hours of data with this trigger, recording about 30,000 events on tape. The majority of the triggers were due to cosmic rays, beam-gas events, and debris from upstream interactions.

Our analysis selected events with a vertex with exactly 2 tracks within 2 cm of the centerline of the TPC, and with $|z| < 2$ m. The track dE/dx were required to be consistent with pions. Electrons and pions can be separated for $p < 140$

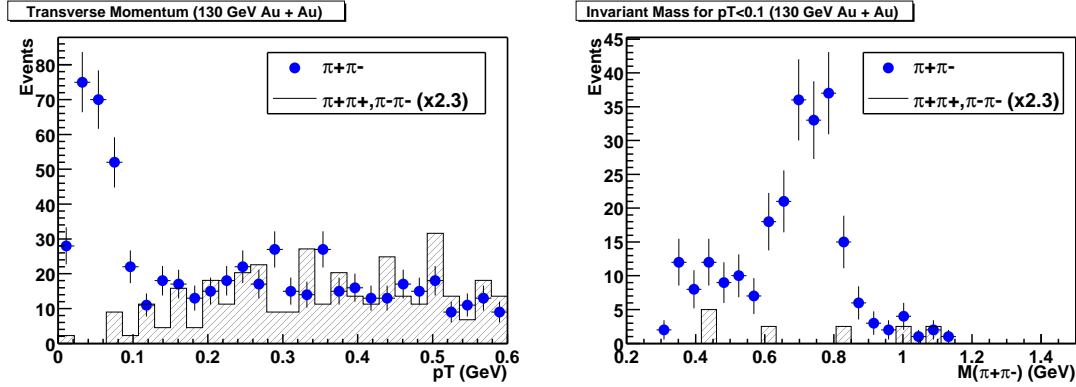


FIGURE 3. (a) The p_T spectrum for minimum bias 2-track events. (b) The $m_{\pi\pi}$ spectrum of 2-track events with $p_T < 100$ MeV/c. The points are oppositely charged pairs, while the histograms are the like-sign background, scaled up by a factor of 2.3.

MeV/c. At higher momenta the two dE/dx bands overlapped. Finally, to reject the remaining cosmic rays, we require the events to have a 3-dimensional opening angle greater than 3 radians (i.e. they must not be perfectly back-to-back).

Fig. 2(a) shows the pair p_T spectrum of the selected unlike-sign (dots - net charge 0) and like-sign pairs (histograms). The unlike pairs are strongly peaked for $p_T < 100$ MeV/c. This is consistent with production that is coherent with both nuclei; events with $p_T < 100$ MeV/c are considered our signal. The like-sign pairs have no such enhancement, and serve as a background sample. The like-sign pairs have been normalized to match the unlike-sign in the signal-free region $250 \text{ MeV} < p_T < 500 \text{ MeV}$; this entailed scaling them up by a factor of 2.1.

Fig. 2(b) shows the invariant mass of the pairs with $p_T < 100$ MeV/c. The points are the unlike-sign events, while the hatched histogram are the scaled like-sign pairs. The like-sign pairs are concentrated at relatively low masses, while the net charge 0 pairs are peaked around the ρ mass. The asymmetric peak is well fit by Eq. (1), with $|B/A|$ similar to that found by the ZEUS collaboration for $\gamma p \rightarrow \rho p$ [15][16]. However, some of the events in the low-mass shoulder are likely due to e^+e^- pairs; subtracting this background will decrease $|B/A|$. There is no evidence for any neutrons in the ZDC data from these events.

ρ^0 WITH NUCLEAR EXCITATION.

Data on ρ production accompanied by mutual nuclear excitation were collected with the minimum bias trigger. This trigger required that signals from one or more neutrons be detected in each ZDC.

The event selection for this analysis was the same as for the topologically triggered sample. Fig. 3a shows the p_T distribution of the track pairs, and Fig. 3b shows the invariant masses of the $\pi\pi$ combinations with $p_T < 100$ MeV/c. The overall background is slightly lower than for the topological trigger, but the composition is quite different. Here, the like-sign pair background was scaled up by a factor of 2.3 to match the like-sign pairs in the region $250 \text{ MeV} < p_T < 500 \text{ MeV}$. Compared to the topologically triggered sample, the backgrounds from beam gas events and cosmic rays are greatly reduced, but the contribution due to grazing nuclear collisions is larger. Despite these differences, the ρ mass peak has a similar shape and $|B/A|$ as the topologically triggered data.

ELECTRON-POSITRON PAIR PRODUCTION

This analysis selected events where both particles were identified as leptons (and hence with $p < 140$ MeV/c). Leptons from these are shown by the triangles in Fig. 4a. Fig. 4b shows the p_T spectrum for events with two identified electrons with $p_T < 140$ MeV/c. There is a clear peak for pair $p_T < 50$ MeV/c. The photon $p_T \sim \hbar c/b$ (considerably less than the $\hbar c/R$ sometimes quoted), so the p_T spectrum is consistent with the expected photon p_T .

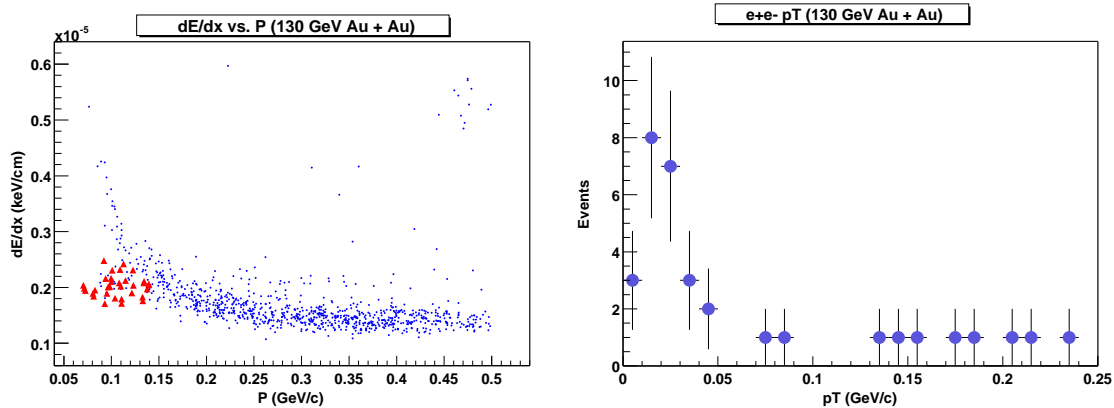


FIGURE 4. (a) The dE/dx of tracks in the 2-track, minimum bias sample. The points are from all tracks, while the triangles are from events where both particles are identified as electrons. (b) The p_T spectrum of events where both particles are identified as electrons.

CONCLUSIONS

We have observed for the first time the reactions $Au + Au \rightarrow Au + Au + \rho^0$, $Au + Au \rightarrow Au^* + Au^* + \rho^0$ and $Au + Au \rightarrow Au^* + Au^* + e^+e^-$. The final states have a small perpendicular momentum, showing their coherent coupling to both nuclei.

In 2001, RHIC is running at $\sqrt{s_{NN}} = 200$ GeV and will attempt to reach full design luminosity, with shorter beam bunches ($\sigma_z \sim 20$ cm). STAR has added several new detector elements: a silicon vertex tracker and forward TPCs, along with an electromagnetic calorimeter. In addition, the STAR trigger will be able to take topological triggers in parallel with central collision triggers. Together, these improvements should give us several orders of magnitude more data. We expect to study additional final states, including the J/ψ and the $\pi^+\pi^-\pi^+\pi^-$ final states of the $\rho^*(1450)$ and $\rho^*(1700)$, and to study ρ production with greater precision and increased angular acceptance. This will allow us to study the interference between the two vector meson production sites. We will also begin to study two-photon production of scalar and tensor mesons.

REFERENCES

1. G. Baur, K. Hencken and D. Trautmann, J. Phys. G**24**, 1657 (1999); C. A. Bertulani and G. Baur, Phys. Rep. **163**, 299 (1988).
2. C. A. Bertulani and F. Navarra, nucl-th/0107035.
3. J. Nystrand and S. Klein, nucl-ex/9811007, in *Proc. Workshop on Photon Interactions and the Photon Structure* eds. G. Jarlskog and T. Sjöstrand, Lund, Sweden, Sept., 1998.
4. S. Klein and J. Nystrand, Phys. Rev. **C60**, 014903 (1999).
5. P. Söding, Phys. Lett. **19**, 702 (1966).
6. S. Klein and J. Nystrand, Phys. Rev. Lett. **84**, 2330 (2000).
7. A. J. Baltz, M. J. Rhoades-Brown and J. Weneser, Phys. Rev. **E 54**, 4233 (1996).
8. A. J. Baltz, C. Chasman and S.N. White, Nucl. Instrum. & Meth. **A417**, 1 (1998); I. Pschenichnov *et al.*, Phys. Rev. **C64**, 024903 (2001).
9. M. Vidovic, M. Greiner and G. Soff, Phys. Rev. **C48**, 2011 (1993).
10. S.N.Gupta, Phys. Rev. **99**, 1015 (1955).
11. K. Hencken, D. Trautmann and G. Baur, Z. Phys **C68**, 473 (1995).
12. H. Wieman *et al.*, IEEE Trans. Nucl. Sci. **44**, 671 (1997).
13. C. Adler *et al.*, Nucl. Instrum & Meth. **A461**, 337 (2001).
14. J. S. Lange *et al.*, Nucl. Instrum. Meth. **A453**, 397 (2000).
15. J. Breitweg *et al.*, Eur. Phys. J **C2**, 247 (1998).
16. S. Klein, nucl-ex/0104016, presented at the 17th Winter Wkshp. on Nuclear Dynamics, Park City, UT, USA, March 10-17, 2001. To appear in the proceedings.